ACS Sustainable Chemistry & Engineering

pubs.acs.org/journal/ascecg

Research Article

# Fluorescence Labeling of Technical Lignin for the Study of Phenolic Group Distribution as a Function of the Molecular Weight

Anika Salanti, Marco Orlandi,* and Luca Zoia

Cite This: *ACS Sustainable Chem. Eng.* 2020, 8, 8279−8287

Read Online

ACCESS | Metrics & More | Article Recommendations | Supporting Information

**ABSTRACT:** A novel analytical approach based on fluorescence labeling was developed in the effort to increase the understanding of phenolic group distribution in technical lignins. Selective derivatization with a fluorophore (dansyl chloride) of lignin phenolic functionalities was quantitatively achieved under mild reaction conditions. Reference acetylated lignin and labeled lignin were analyzed by gel permeation chromatography (GPC) coupled to a UV−vis detector (set at 280 nm) and a fluorescence detector ($\lambda$ excitation: 390 nm, $\lambda$ emission: 550 nm) to discern the dansyl-linked phenol response from the lignin aromatic skeleton input. After data elaboration, valuable information about the phenolic group distribution as a function of molecular weight for different technical lignins was gathered. This novel analytical approach is applied to model lignin polymer thermal protection properties, a useful parameter in lignin valorization strategies.

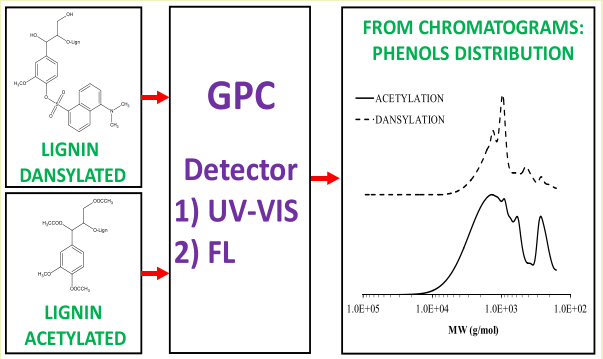


**KEYWORDS:** *Technical lignin, Phenol, Dansyl, Fluorescence, Molecular weight*



## INTRODUCTION

Lignins are three-dimensional, heterogeneous, and irregular polyphenolic macromolecules and the second most abundant natural polymer after cellulose. Along with hemicelluloses, these biopolymers constitute the so-called lignocellulosic materials. Lignin is constituted by three phenolic monomers, named *p*-hydroxyphenyl (H), guaiacyl (G), and syringyl (S) units when linked into the lignin polymer through ether and carbon−carbon bonds.[1] The structure of a lignin, as well as the amounts of the three monomeric units, depend on the botanical origin and the type of lignocellulosic biomass. Approximately 50 million tons of technical lignins are annually produced from spent pulping liquors, mainly from the sulphite and kraft processes.[2] During the pulp and paper production, intermolecular linkages are broken and modified to separate lignin from the lignocellulosic composite, and the already complicated lignin structure is strongly affected by these treatments.[3] The heterogeneity of the resulting technical lignin is the major drawback for its valuable valorization.[4] Several papers were focused on different fractionation approaches to extract more homogeneous lignin preparation in terms of molecular weight and functional group distribution.[5] It was demonstrated that sequential ultrafiltration of kraft lignin is able to fractionate and elucidate molar-mass-dependent changes in lignin structure and characteristics, revealing that the smaller fractions are also the richest in phenolic groups.[6−8] Selective solvent extraction, the oldest fractionation techniques described, takes advantage of the different solubilities of lignin in solvents with varying polarity.[9] In general, the lower the solvent polarity, the lower the average molecular weight of the fraction and the larger the phenolic content.[10−12] Fractionation by successive precipitation, obtained either by a stepwise reduction of the pH value of black liquor or especially by the addition of a nonsolvent to an organic lignin solution, generally results in a high lignin yield and highly monodispersed fractions.[13−15]

Despite these efforts, a strong contribution in the field of the analytical chemistry of lignin is still necessary to deeply understand and completely control lignin up-grading. As reported by Potthast and co-workers, "in general, from an analytical point of view, the understanding of technical lignins is set back by the common analysis approach—putting together fragments with known structural features and perhaps some newly identified motifs and complementing this by analyzing many functional groups. However, we have not yet arrived at a stage where we can state that we comprehend the whole picture of this fascinating molecule".[7] The presented study is focused on the possibility to obtain a precise knowledge about the distribution of phenolic groups in technical lignins as a function of their molecular weight, avoiding the need of a preliminary

Received: February 28, 2020
Revised: May 7, 2020
Published: May 11, 2020







https://dx.doi.org/10.1021/acssuschemeng.0c01571
*ACS Sustainable Chem. Eng.* 2020, 8, 8279−8287

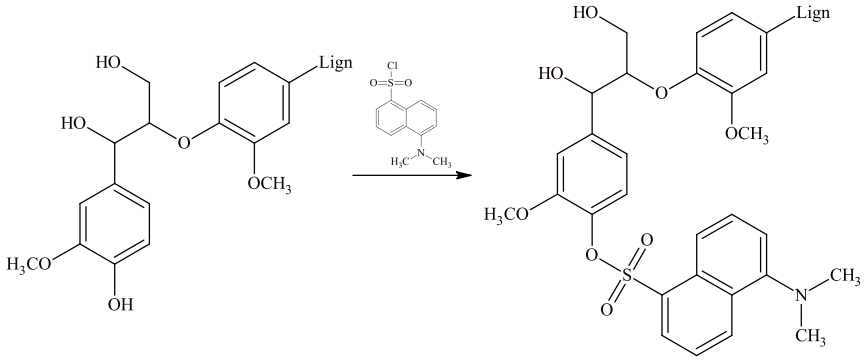


**Figure 1.** Dansylation reaction for a typical $\beta$-O-4 structure of a guaiacylic nature.

lignin fractionation process. Fractionation procedures are indeed expensive in terms of time, resources, and effort, whereas according to the method herein described, a GPC analysis performed on the lignin sample as a whole might be enough to select a specific fraction of interest. Otherwise, the generally proposed workflow involving fractionation followed by fraction analysis might be replaced by the inverse, plainer approach analysis fractionation. In particular, the proposed analytical method is based on the selective fluorescence labeling of lignin phenolic moieties with dansyl chloride. The phenols were chosen as the main representative and are a versatile functional group on account of their properties and easiness of conversion to other reactive species. The selectivity and yield of the labeling reaction were determined by quantitative phosphorylation of phenols followed by $^{31}$P NMR.[16] The fluorescence-labeled lignin, along with the acetylated reference, was then analyzed by gel permeation chromatography (GPC) and performed on an instrument connected to a UV−vis (GPC−UV) and a fluorescence (GPC−FL) detector. The comparison between the acetylated and dansylated GPC profiles, properly evaluated and computed, returned helpful information about phenol concentration over different molecular weight ranges.

## EXPERIMENTAL SECTION

**Reagents and Materials.** All solvents and reagents were purchased from Sigma-Aldrich Italia and used as received. Technical lignins from the kraft process (softwood kraft, SWK; hardwood kraft, HWK), soda pulping (soda grass, SG), and steam explosion (wheat straw, $WS_{SE}$) were kindly provided by local factories. The $WS_{SE}$ was further purified by an acidic−basic treatment according to the optimized conditions described by Zoia et al.[17]

**Lignin Acetylation.** Lignin samples (ca., 50 mg) were acetylated using 1:1 pyridine/acetic anhydride mixtures (2 mL, 40 °C, 24 h) and recovered by stripping with EtOH, toluene, and chloroform before being subjected to GPC analysis.

**Lignin Dansylation.** In a typical experimental procedure, 100 mg of lignin and 5 mg of tetrabutylammonium bromide (TBAB) were dissolved in 20 mL of carbonate buffer solution (pH 10, 0.1 M) and heated to 50 °C in an oil bath. A certain amount of dansyl chloride (20% molar excess to the total phenolic content as calculated from $^{31}$P NMR) was then solubilized in acetonitrile (10 mL) and added to the lignin solution. The mixture was reacted for 90 min at 50 °C under vigorous stirring. At the end of the reaction, dansylated lignin was recovered by centrifugation (4000 rpm, 10 min, two cycles washing with acidic water) after regeneration in cold acidic water (HCl, 0.1 M). For the purpose of this work, the yield of the dansylation reaction was evaluated by $^{31}$P NMR as the % of reacted phenols. (Full spectra are provided as Supporting Information.)

**Model Compound Synthesis.** Dimeric model compounds of vanillyl alcohol (MW 154.2 g/mol) and isoeugenol (MW 164.2 g/mol) were obtained via enzymatic oxidative coupling.[18] Monomer (500 mg) was dissolved in a 3:1 phosphate buffer/dioxane solution (phosphate buffer, 0.05 M, pH 6.0). Afterward, 1 mg of type VI-A horseradish peroxidase (activity: 950−2000 units/mg of solid using ABTS) was added. The amount of oxidant (hydrogen peroxide, $H_2O_2$, 30% w/v in water) was calculated according to a 1:0.5 model compound/$H_2O_2$ ratio, prepared as a 3% solution in water and added to the reaction mixture under gentle stirring in five aliquots, every 5 min, over an average period of 30 min. During the addition of the oxidant, the reaction was monitored by thin layer chromatography (TLC, eluent 7:3 hexane/ethyl acetate). The products were extracted into ethyl acetate, washed twice with slightly acidic water, dried over anhydrous sodium sulfate, and vacuum-dried. The crude was purified on a silica flash column (silica gel 60, 230−400 mesh ASTM, Merck) eluted with 6:4 hexane/ethyl acetate. For the purpose of this work, both the dimer and the residual monomer were recovered and used as a representative simple mixture to validate the chromatographic method developed. The linkage distributions of the oxidation products were detected by $^{1}$H NMR and $^{13}$C NMR. The average phenolic content of the mixtures was assessed by quantitative $^{31}$P NMR analysis. (Spectra are provided as Supporting Information.)

**Model Compound Dansylation.** The dansylation reaction on model compounds was accomplished using the same conditions described above for lignin except that, after the addition of the reaction mixture to cold acidic water, the pH was adjusted to 3 to optimize the product precipitation, and then, the dansylated model compounds were extracted in ethyl acetate, anhydrified over sodium sulfate, and rotary evaporated. The conservation of the intact dansyl units was verified by $^{1}$H NMR and $^{13}$C NMR. The yield of the reaction, in terms of reacted phenolic functionality, was assessed by $^{31}$P NMR. (Spectra are provided as Supporting Information.)

**$^{31}$P NMR Analyses.** Quantitative $^{31}$P NMR analyses were performed according to a well-established procedure[16] using 2-chloro-4,4,5,5-tetramethyl-1,3,2-dioxaphospholane as a phosphorus derivatizing agent. The $^{31}$P NMR data reported in this paper are the average of three experiments. The maximum standard deviation was 0.02 mmol/g, while the maximum standard error was 0.01 mmol/g.

**GPC−UV−Fluorescence Analysis.** GPC analyses were performed on an Agilent 1260 Infinity liquid chromatography system, equipped with an autosampler (Agilent 1260 Vialsampler, injection volume 25 $\mu$L), and connected in series to an Agilent 1260 DA VL detector (set at 280 nm) and an Agilent 1260 FL detector ($\lambda$ excitation: 390 nm, $\lambda$ emission: 550 nm for all samples). The GP column system was composed as follows (according to the solvent flow direction): Agilent PLgel 5 $\mu$m, 500 Å, Agilent PLgel 5 $\mu$m, 1000 Å, and Agilent PLgel 5 $\mu$m, 10 000 Å. Samples were dissolved in tetrahydrofuran (THF, accurately prepared at the concentration of 1 mg/mL starting from more concentrated stock solutions) and analyzed using THF as an eluent (Fluka 99.8%) at a flow rate of 1 mL/min. PL polymer standards of polystyrene from Polymer Laboratories were used for calibration. The evaluation of the number-average molecular weight ($M_n$) and the weight-average molecular weight ($M_w$) of the acetylated lignin samples was performed. The peak molecular weight $M_p$ is defined as the molecular weight of the species with maximum absorbance. Moreover,


https://dx.doi.org/10.1021/acssuschemeng.0c01571
ACS Sustainable Chem. Eng. 2020, 8, 8279−8287

Table 1. Mass Ratio[a], Experimental Quantification ($^{31}$P NMR)[b] for SWK, HWK, SG, and $WS_{SE}$ Lignins before and after Dansylation, and Percentage of Conversion for Aliphatic Alcohols, Carboxylic Acids, and Phenols

| | SWK | SWK dans | HWK | HWK dans | SG | SG dans | $WS_{SE}$ | $WS_{SE}$ dans |
|---|---|---|---|---|---|---|---|---|
| mass ratio | 0.51 | | 0.60 | | 0.55 | | 0.69 | |
| aliph−OH ($^{31}$P NMR, mmol/g) | 2.02 (1.03) | 0.82 | 1.12 (0.67) | 0.56 | 1.84 (1.01) | 0.77 | 2.02 (1.39) | 1.10 |
| aliph−OH conversion (%) | 20 | | 17 | | 24 | | 21 | |
| COOH ($^{31}$P NMR, mmol/g) | 0.52 (0.27) | 0.28 | 0.38 (0.23) | 0.21 | 1.04 (0.57) | 0.34 | 0.68 (0.47) | 0.38 |
| COOH conversion (%) | −5 | | 8 | | 40 | | 19 | |
| PhOH ($^{31}$P NMR, mmol/g) | 4.39 (2.24) | 0.15 | 2.93 (1.76) | 0.15 | 3.71 (2.04) | 0.09 | 2.09 (1.44) | 0.07 |
| PhOH conversion (%) | 93 | | 91 | | 96 | | 95 | |

[a]Starting weight/final weight of lignin after the dansylation reaction. [b]Expressed as mmol/g.

the ratio $I = M_w/M_n$, defined as the polydispersity index, was also calculated. The $M_n$, $M_w$, and $M_p$ values reported are the average of three analyses (standard error $M_w$: 1000 g/mol; $M_n$, $M_p$: 100 g/mol). The phenol content, calculated from GPC−FL data, reported in this paper is the average of three experiments. The maximum standard deviation was 0.2 mmol/g, while the maximum standard error was 0.1 mmol/g.

## RESULTS AND DISCUSSION

**Dansylation Reaction.** As reported in the Experimental Section, lignin samples were labeled with dansyl chloride (Figure 1) and then characterized by $^{31}$P NMR in order to study the yield and the selectivity of the reaction (full spectra provided as Supporting Information).

The results after the dansylation reaction on the SWK, HWK, SG, and $WS_{SE}$ lignins are reported in Table 1. The reaction sites taken in consideration were alcohols, carboxylic acids, and phenols. Concerning HW and SW kraft lignin, the presence of sulfur had also to be considered: kraft lignin samples could contain around 2−3% of S, roughly 10% of which is in the form of thiols.[14] Anyway, the formation of thiosulfonate lignin derivatives did not seem feasible according to the applied reaction conditions. For the aim of this work, first a mass ratio for each lignin was calculated as the ratio between the starting weight and the final weight of lignin after the dansylation reaction (Table 1, first line). The experimental mass ratios were in line with the theoretical values calculated by adding 233.3 g/mol (the mass of dansyl unit) for each phenolic functionality, supposing that phenols were the only reactive group and assuming a 100% conversion (0.51 vs 0.49 for SWK, 0.60 vs 0.59 for HWK, 0.55 vs 0.53 for SG, and 0.67 vs 0.69 for $WS_{SE}$).

The mass ratios were then used to assess the reliability and selectivity of the dansylation reaction. The comparison between the experimental quantification in mmol/g, obtained by the $^{31}$P NMR of aliphatic alcohols and carboxylic acids (second and fourth lines, Table 1) before (corrected using the mass ratios and reported in bracket) and after dansylation, resulted in a satisfying match between the two values. The dansylation reaction occurred mainly at the phenolic sites and the total amount of phenols (sixth line, Table 1) detected after the derivation approached zero for every sample. The percentages of the conversion were used to evaluate of the actual yield of the dansylation reaction (always >90%). In conclusion, the described labeling reaction was sufficiently selective and complete and was considered a good candidate for the study of lignin phenolic group distribution.[19]

**Chromatographic Data Elaboration.** GPC chromatograms were acquired on acetylated and dansylated specimens as both UV (280 nm) and fluorescence ($\lambda$ excitation: 390 nm, $\lambda$ emission: 550 nm) profiles to gain information about phenol distribution in the examined lignin samples against the lignin skeleton response. Fluorescence full spectra of the dansylated lignin samples are reported in the Supporting Information. The same approach was used in the elaboration of model compound chromatograms. A basic assumption was made on the behavior of the molar extinction coefficient and the fluorescence intensity at the variation of the molecular weight: both were considered constant and independent from the species constituting acetylated and dansylated lignin samples. This means that the UV response of lignin and the fluorescence response of dansyl groups linked to aromatic rings were considered not to be affected by changes in the molecular weight and, especially, by the variegated chemical structure offered by lignin.

In this view, the four chromatograms obtained after GPC analysis were exploited as follows

(1) The UV profile of a generic acetylated lignin sample was used to determine the representative weight fraction of a specific molecular weight range (ranges $b \rightarrow a$ taken as follows: >10 000, 10 000−5000, 5000−3000, 3000−2000, 2000−1000, 1000−160 g/mol). Accordingly, the total UV absorbance calculated over a specified range $\sum_{n=a}^{b} \mathrm{Abs}(n)$ was divided by the total UV absorbance calculated over the whole molecular weight distribution $\sum_{n=160}^{10\,000} \mathrm{Abs}(n)$ according to eq 1

$$\text{g lignin}(b \rightarrow a) = \frac{\sum_{n=a}^{b} \mathrm{Abs}(n)}{\sum_{n=160}^{10\,000} \mathrm{Abs}(n)} \quad (1)$$

For the model mixtures, the integration was performed on the resolved peaks instead of molecular weight ranges.

(2) The fluorescence profile of a generic acetylated lignin sample was used to correct the fluorescence signal of the corresponding dansylated specimen as follows: the acetylated lignin chromatogram was normalized using the proper weight conversion factor (whose calculation has been described in the previous section) and then subtracted from the fluorescence chromatogram of the analogous dansylated sample to remove the autofluorescence contribution of the lignin skeleton. Autofluorescence phenomena in lignin are promoted by the occurrence of aromatic structures such as phenylcoumarones and stilbenoids.[20,21] When the autofluorescence of nondansylated lignin samples and model compounds was negligible, this step was skipped.

(3) The UV profile of a generic dansylated sample (Supporting Information, in comparison with the corresponding acetylated UV profile) was used to estimate the change in the hydrodynamic volume of the corresponding lignin after dansylation. Since the shift toward higher molecular weights after the insertion of the



https://dx.doi.org/10.1021/acssuschemeng.0c01571
ACS Sustainable Chem. Eng. 2020, 8, 8279−8287

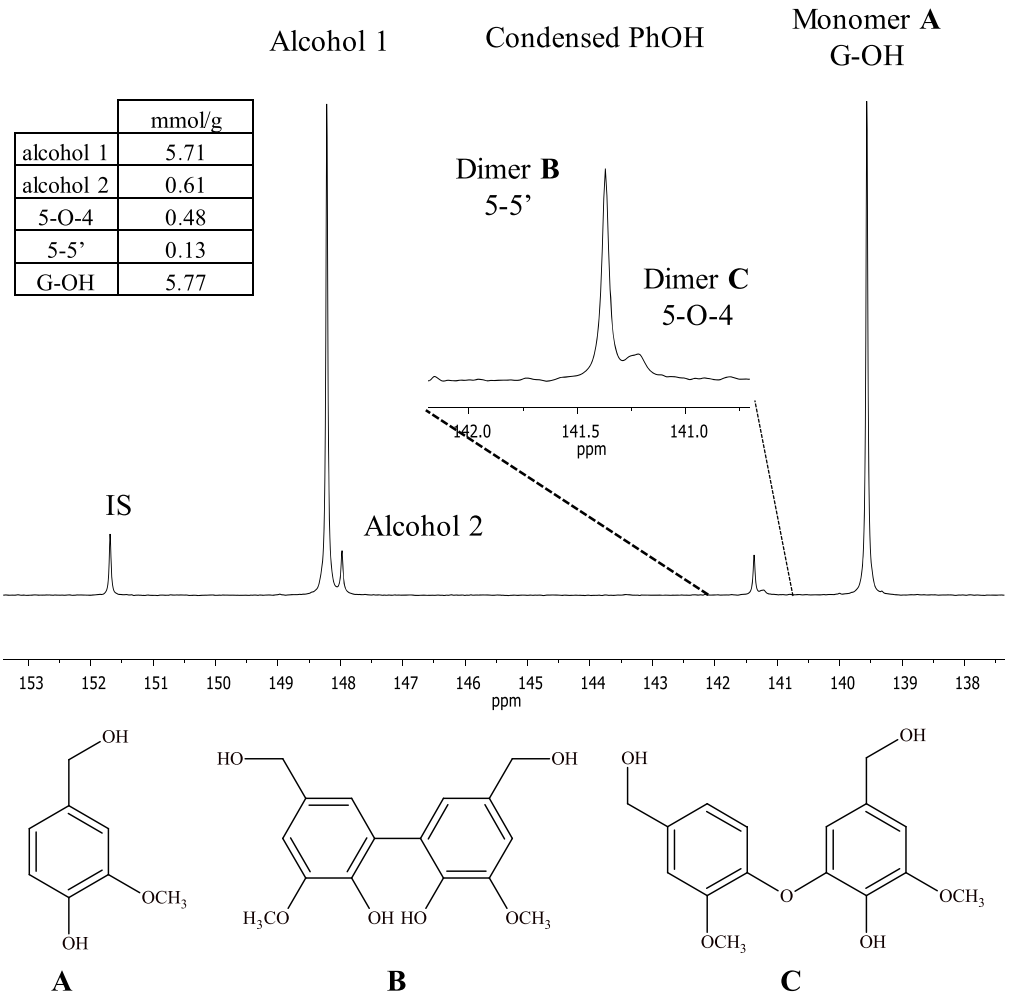


**Figure 2.** $^{31}$P NMR spectrum and molecular structures of the vanillyl alcohol oxidation products individuated in the Model 1 mixture.

dansyl group is more marked for low molecular weight species, the integration range of 1000−160 g/mol in the acetylated profile was modified into 1250−160 g/mol for the dansylated profile to take in account this effect. The other ranges were not modified.

(4) The elaboration of the fluorescence profile of a generic dansylated sample provided the representative phenolic molar fraction referred to a specified molecular weight range (ranges $b \rightarrow a$ are the same listed at point 1). The phenolic molar fractions were obtained according to the following relationship 2

$$\text{PhOH mmol}(b \rightarrow a) = \frac{\sum_{n=a}^{b} \text{Fluo}(n)}{\sum_{n=160}^{10\,000} \text{Fluo}(n)} * \text{PhOH mmol(tot)} \quad (2)$$

where $\sum_{n=a}^{b} \text{Fluo}(n)$ is the fluorescence intensity over a specified molecular weight range $b \rightarrow a$; $\sum_{n=160}^{10\,000} \text{Fluo}(n)$ is the total fluorescence intensity calculated over the whole molecular weight range; and PhOH mmol(tot) is the average content of phenols for a given 1 g sample, as obtained from the $^{31}$P NMR quantification.

The obtained data are meant to be used in the eq 3

$$\text{PhOH}\frac{\text{mmol}}{\text{g}}(b \rightarrow a) = \frac{\text{mmol PhOH}(b \rightarrow a)}{\text{g lignin}(b \rightarrow a)} \quad (3)$$

a molecular-weight-range-dependent version of the well-known equation[22] usually exploited for the average assessment of lignin phenolic moiety quantification. Again, for the model mixtures, the integration was performed on the resolved peaks instead of molecular weight ranges.

**Application to Model Compounds.** The procedure described so far was applied on simple mixtures obtained from the enzymatic dimerization of two model compounds, vanillyl alcohol and isoeugenol. The aim of this first application was (i) to confirm the reaction selectivity on phenols; (ii) to detect the intact dansyl unit on the lignin-like structures; and (iii) to assess the linear correlation between the phenol content and the dansyl fluorescence. The two mixtures were accordingly analyzed by $^{31}$P NMR and GPC−UV−fluorescence. Figure 2 displays the $^{31}$P NMR spectra of the mixture obtained after flash-column purification of vanillyl alcohol (**A**) enzymatic coupling. The presence of dimer 5-5′ structure (**B**) was confirmed by NMR (proton and carbon spectra are reported in the Supporting Information), while the dimer 5-O-4 (**C**) was detected by GPC and $^{31}$P NMR as well as literature accounts.[23] The phosphorus spectrum highlighted the presence of two peaks related to


https://dx.doi.org/10.1021/acssuschemeng.0c01571
ACS Sustainable Chem. Eng. 2020, 8, 8279−8287

hydroxyl groups (named Alcohol 1 and Alcohol 2) and three peaks related to phenols. The signals Alcohol 1 and Alcohol 2 were interpreted as unreacted and dimeric vanillyl alcohol, respectively, whereas the peaks in the range of 138−140 ppm were ascribed to 5-5′ and 5-O-4 dimers (**B** and **C**) and unreacted vanillyl alcohol (monomer **A**, G−OH). The total amount of phenols detected by $^{31}$P NMR analysis was 6.39 mmol/g; the hydroxyl distribution among the species is reported in the table inserted in Figure 2.

The Model 1 mixture was then dansylated and analyzed by $^{31}$P NMR, which confirmed a 100% dansylation yield of phenols (Supporting Information), and then by GPC. In Figure 3 is reported the GPC−UV profile of the nondansylated mixture along with the GPC−FL profile of the mixture after dansylation.

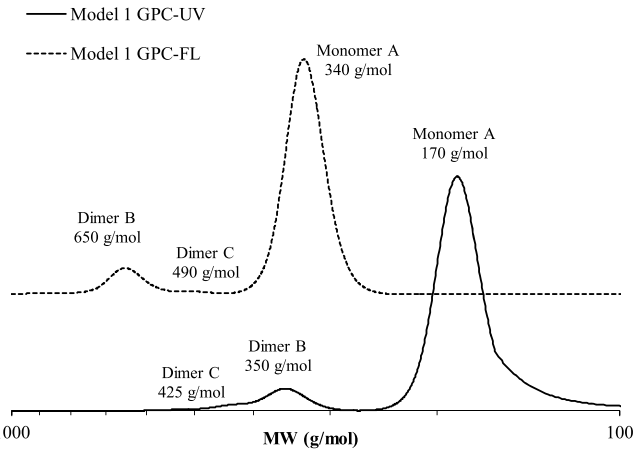


**Figure 3.** GPC−UV (solid line) and GPC−FL (dashed line) profiles of the Model 1 mixture.

As already found in the $^{31}$P NMR spectrum, the GPC−UV profile (solid line) showed the presence of two dimeric structures (**B** at around 350 g/mol and **C** at around 425 g/mol, visible as a shoulder, assigned to the 5-5′ and the 5-O-4 dimer, respectively, 306.2 g/mol) generated by the enzymatic dimerization of the monomer (**A**, around 170 g/mol). In the GPC−FL chromatogram (dashed line) were recognizable the dansylated vanillyl alcohol (peak **A**, around 340 g/mol), the monodansylated 5-O-4 dimer (peak **C**, ca., 490 g/mol), and the didansylated 5-5′ dimer (peak **B**, ca., 650 g/mol). It is worth noticing that the reverse elution order was in line with the stoichiometry of the dansylation reaction, i.e., one dansyl unit for the 5-O-4 dimer (306 + 233 = 539 g/mol) vs two dansyl units for the 5-5′ dimer (306 + 233 + 233 = 772 g/mol).

The results of the elaboration of the chromatographic data, performed as previously described, are reported in Table 2. In the first column we reported the quantification from $^{31}$P NMR analyses, in the second column, we reported the weight fraction from the integration of the GPC−UV chromatogram of the undansylated mixture, in the third column, we reported the PhOH content from the integration of the GPC−FL chromatogram of dansylated material, in the fourth column, we reported the PhOH content calculated by dividing the PhOH from GPC−FL by the weight fraction, and in the last column, we reported the theoretical phenol content of each chemical species. Interestingly, through the elaboration of the GPC−FL profile, the mmol of phenols contained in the different fractions of the mixture were in good agreement with the $^{31}$P NMR data (compare first and third columns, Table 2). After normalization

**Table 2. GPC−UV and GPC−FL Elaboration Output for Each Fraction of Model 1 Mixture: Weight Fraction (w/w), Phenol Content[a] as Obtained from GPC−FL Profile Elaboration, Phenol Content in mmol/g, and Theoretical Phenol Content in mmol/g[b]**

| | PhOH $^{31}$P NMR (mmol/g) | weight fraction (w/w) | PhOH calc. GPC (mmol) | PhOH calculated (mmol/g) | PhOH theor. (mmol/g) |
|---|---|---|---|---|---|
| monomer **A** | 5.78 | 0.856 | 5.7 | 6.7 | 6.49 |
| dimer **B** (5-5′) | 0.48 | 0.088 | 0.5 | 6.2 | 6.54 |
| dimer **C** (5-O-4) | 0.13 | 0.055 | 0.1 | 2.4 | 3.26 |

[a]Calculated for 1 g of sample. [b]$^{31}$P NMR total phenol content equal to 6.39 mmol/g.

on the weight fraction, the absolute phenol content for each fraction was obtained in sound agreement with the theoretical mmol/g calculated for each structure (compare fourth and fifth columns, Table 2).

The same procedure was applied to the mixture recovered after flash-column purification of isoeugenol enzymatic coupling. According to GPC and NMR analyses (Supporting Information), along with unreacted residual monomer (**A**), the main product was the $\beta$-5 dimer (Figure 4, dimer **B**).[24] The total amount of phenols detected by $^{31}$P NMR was 4.93 mmol/g; their amount after dansylation was null (Supporting Information).

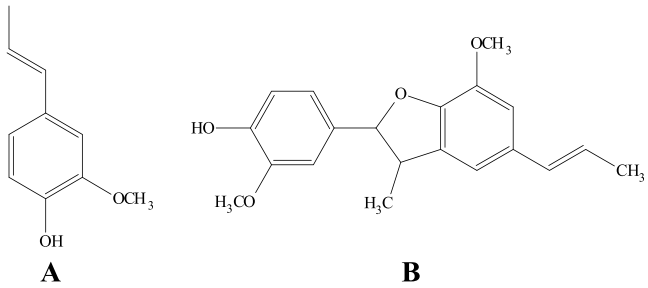


**Figure 4.** Molecular structure individuated in Model 2.

Figure 5 reports the GPC−UV profile of the nondansylated mixture along with the GPC−FL profile after dansylation. In the GPC−UV profile (solid line) was recognizable the peak of the monomer (**A**) at around 200 g/mol, the peak of the $\beta$-5 dimer (**B**) at around 400 g/mol, and some other unresolved peaks between 600 and 1000 g/mol arising from oligomeric structures (**C**). After dansylation (dashed line), the peaks were shifted to higher molecular weights; their elution order was consistent with the reactivity of uncondensed structures (one dansyl unit per molecule).

As already occurred for vanillyl alcohol and its dimers, the elaboration of the GPC−UV and GPC−FL profiles of the Model 2 mixture resulted in a phenol quantification associated with the monomer, dimers, and oligomers that is in good agreement with the calculated theoretical values (Table 3).

In light of the results of these experiments, it was possible to confirm that the dansyl unit, even if in the presence of intermonomeric lignin-like bonds (such as the 5-5′, 5-O-4, and $\beta$-5 linkages), is not subjected to quenching phenomena. Moreover, a linear correlation between the dansyl fluorescence and the phenol concentration was found. Both these findings are


https://dx.doi.org/10.1021/acssuschemeng.0c01571
ACS Sustainable Chem. Eng. 2020, 8, 8279−8287

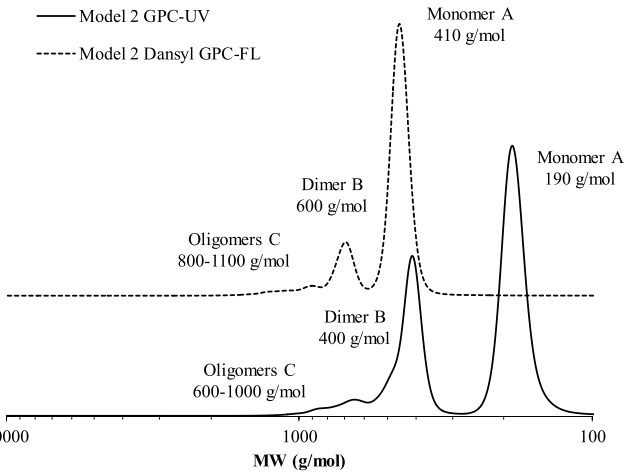


**Figure 5.** GPC−UV (solid line) and GPC−FL (dashed line) profiles of Model 2 mixture.

**Table 3. GPC−UV and GPC−FL Elaboration Output for Each Fraction of Model 2 Mixture: Weight Fraction (w/w), Phenol Content[a] as Obtained from GPC−FL Profile Elaboration, Phenol Content in mmol/g, and Theoretical Phenol Content in mmol/g[b]**

| | PhOH $^{31}$P NMR (mmol/g) | weight fraction (w/w) | PhOH calc. GPC (mmol) | PhOH calculated (mmol/g) | PhOH theor. (mmol/g) |
|---|---|---|---|---|---|
| monomer **A** | total content: | 0.55 | 3.4 | 6.3 | 6.10 |
| dimer **B** ($\beta$-5) | 4.97 (signals overlapped) | 0.27 | 0.9 | 3.2 | 3.07 |
| oligomer **C** | | 0.16 | 0.3 | 1.9 | 2.05 |

[a]Calculated for 1 g of sample. [b]$^{31}$P NMR total phenol content equal to 4.97 mmol/g.

of importance for the application of the method herein developed.

**GPC Analyses.** GPC profiles of all the examined lignins, under UV−vis detection (280 nm) after acetylation and under fluorescence detection ($\lambda$ excitation: 390 nm, $\lambda$ emission: 550 nm) after dansylation, are reported in Figure 6. In order to confirm the linear correlation between the dansyl fluorescence and the phenol concentration, the integration of the GPC−FL profiles of dansylated lignins (in A.U.) and $^{31}$P NMR total phenol content (in mmol/g) for all the samples were compared as reported in Supporting Information, and a good linear correlation was found. From a qualitative point of view, the molecular weight distribution of dansylated specimens under fluorescence detection was sharper. In addition, accumulation peaks were diagnostic for the coelution phenomena of lignin molecules with large phenol content. The molecular weight distributions of both the HWK and $WS_{SE}$ lignin before and after dansylation were similarly scattered along the abscissa, while the same chromatograms of the SWK and SG lignin were quite different, characterized by a lower phenol content at high molecular weight. The autofluorescence contribution of the lignin skeleton (profiles not reported) was limited but not negligible for all the samples involved (fluorescence intensity of acetylated vs dansylated samples averagely 1:10).

The calculated phenols content for the four technical lignins over different molecular weight ranges is reported in Table 4. These data were extracted from the GPC chromatograms, as described in the "Chromatographic Data Elaboration" section. In order to give a complete picture, the average molecular weight indexes and labile −OH group distribution data obtained by GPC−UV and $^{31}$P NMR analysis are reported.

The same data can be expressed as the number of phenol functionalities per phenylpropanoidic unit (PhOH/$C_9$, where the molecular weight of the $C_9$ unit was set to 200 g/mol) to quickly evaluate the amount of phenols contained in each fraction. Moreover, this new set of data can be conveniently visualized in Figure 7.

For the SWK and SG lignins, the phenolic distribution over the examined ranges was quite heterogeneous: at high molecular weights, the number of phenol/$C_9$ was low, whereas it rapidly increased for low molecular weights.[25] In particular, the behavior of SWK lignin was remarkable in that the phenol content was higher than 1 PhOH/$C_9$ below 3000 g/mol. It seems like SWK lignin is constituted by different motifs: at higher molecular weight prevails a more native structure, less condensed, whereas at lower molecular weight, residual condensed lignin[26] structures not degraded by the process coexist with "new", condensed structures generated via radical/ionic coupling of lignin fragments released during the kraft treatment.[4,27,28] In order to explain the unexpected phenolic content below 1000 g/mol, also a partial demethoxylation could be considered. These data for a softwood kraft lignin are in good agreement with the data reported by Crestini and Lancefield.[4,27] On the contrary, the HWK lignin showed a more homogeneous phenolic distribution, on average comprising between 0.4 and 0.6 phenols per $C_9$ over the whole examined ranges. All the hardwood lignin fractions seemed to be affected by the kraft process at the same extent, but the pristine syringyl nature of the macromolecules decreased the formation of new condensed structures during kraft pulping. Lastly, the $WS_{SE}$ lignin displayed a lower phenol content over the whole ranges, and especially at higher molecular weights, which was consistent with a mainly uncondensed structure.[29]

This novel analytical approach offers several valuable insights, for example, a tool for researchers to study the lignin chemical modification after extractive processes and to decide the best lignin fraction to select for a particular application. The higher phenolic content at low molecular weights makes the examined softwood kraft lignin a good candidate for an up-grading treatment aimed at the preparation of antioxidant molecules,[30] reactive polyfunctional precursors, and cross-linkers. On the other hand, the investigated hardwood kraft lignin, characterized by a constant phenolic content over its molecular weight distribution, could be easily used without preliminary fractionation process.

As an application, the phenolic group distribution was employed in the forecasting of a particular chemophysical property, the polymer thermal protection, as described by Barana et al.[31] In that paper, the authors found that the ratio between the total phenolic content and the chromatographic peak molecular weight $[PhOH]/M_p$ was linearly correlated to the OIT (oxygen induction time), the protection time measured by DSC (differential scanning calorimetry), on a lignin/natural rubber blend. From the data obtained with GPC−FL analyses, for each lignin specimen (SWK, HWK, SG, and $WS_{SE}$) the ratio between the PhOH ($b \rightarrow a$) content, expressed as mmol/g, and the average molecular weight of the specific molecular weight range ($\overline{MW}_{b\rightarrow a} = (b + a)/2$) was calculated. Then, the theoretical OIT was estimated applying the following linear correlation


https://dx.doi.org/10.1021/acssuschemeng.0c01571
ACS Sustainable Chem. Eng. 2020, 8, 8279−8287

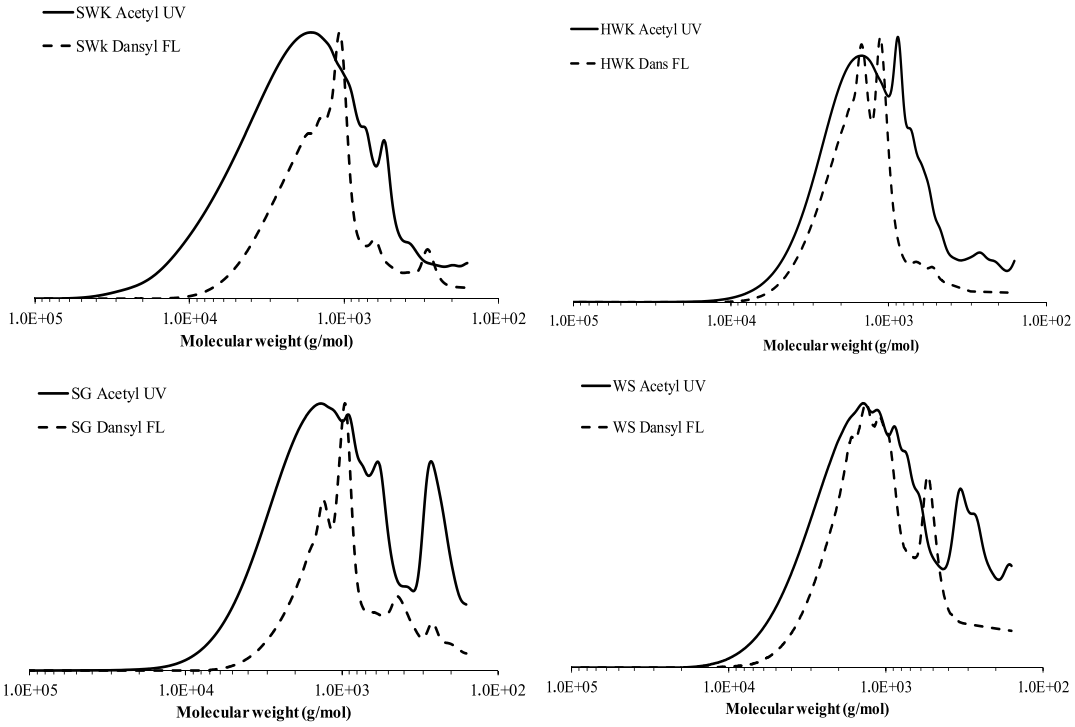


**Figure 6.** Overlapped GPC profiles of acetylated (280 nm, solid line) and dansylated (exc: 390 nm, em: 550 nm, dashed line) SWK, HWK, SG, and $WS_{SE}$ lignins.

**Table 4. GPC Outcomes, $^{31}P$ NMR Characterization, and Phenol Quantification as Calculated from the GPC Fluorescence Profile of SWK, HWK, SG, and $WS_{SE}$ Technical Lignins Expressed as mmol/g at the Specified Molecular Weight Range[a]**

| | SWK | HWK | SG | $WS_{SE}$ |
|---|---|---|---|---|
| $M_n$ | 3030 | 1720 | 1730 | 1700 |
| $M_w$ | 7250 | 2730 | 3360 | 3100 |
| PD | 2.39 | 1.59 | 1.94 | 1.83 |
| −OH (mmol/g) | 2.02 | 1.12 | 1.84 | 2.02 |
| −COOH (mmol/g) | 0.52 | 0.38 | 1.04 | 0.68 |
| PhOH (mmol/g) | 4.39 | 2.93 | 3.71 | 2.09 |
| **mmol/g of PhOH per MW range** | | | | |
| <10 000 g/mol | 0.1 | 0.2 | 0.0 | 0.2 |
| 10 000−5000 g/mol | 1.2 | 1.7 | 0.3 | 0.6 |
| 5000−3000 g/mol | 3.0 | 2.8 | 1.3 | 1.2 |
| 3000−2000 g/mol | 4.6 | 3.3 | 2.5 | 1.9 |
| 2000−1000 g/mol | 4.3 | 2.8 | 3.1 | 1.9 |
| >1000 g/mol | 7.7 | 3.0 | 5.6 | 2.6 |

[a]Standard error = ±0.1 mmol/g.

$$\mathrm{OIT}(b \rightarrow a) = 11\,488\frac{[\mathrm{PhOH}(b \rightarrow a)]}{\bar{M}\bar{W}_{b \rightarrow a}} + 0.2331 \quad (4)$$

and the OIT values obtained were normalized by the weight representativeness of the considered lignin fraction. The sum of these values represented the calculated OITs, and they were compared with the experimental ones.[31] The results are reported in Table 5. Calculated and experimental values are in good agreement, although a general overestimation is observed for calculated OITs.

The data are in line with the results reported in a paper by Sadeghifar et al.,[32] where the authors studied the effect of the acetone-based fractionation of SWK on the $OIT_{temp}$ (oxidation

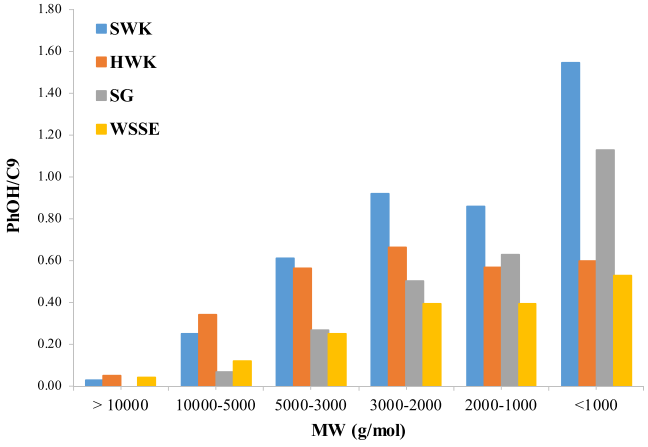


**Figure 7.** $PhOH/C_9$ trend for the examined lignin samples SWK, HWK, SG, and $WS_{SE}$ over the molecular weight ranges considered.

**Table 5. Partial, Calculated, and Experimental OITs for SWK, HWK, SG, and $WS_{SE}$ Lignin**

| | | SWK | HWK | SG | $WS_{SE}$ |
|---|---|---|---|---|---|
| OIT weighed (min) | >10000 | 0.01 | 0.00 | 0.00 | 0.00 |
| | 10000−5000 | 0.24 | 0.07 | 0.03 | 0.04 |
| | 5000−3000 | 1.44 | 0.78 | 0.41 | 0.39 |
| | 3000−2000 | 3.65 | 2.72 | 1.76 | 1.38 |
| | 2000−1000 | 9.54 | 8.28 | 7.59 | 4.84 |
| | <1000 | 34.54 | 19.36 | 43.85 | 20.48 |
| **OIT calculated (min)** | | **49.42** | **31.20** | **53.64** | **27.13** |
| **OIT experimental (min)** | | **44.2** | **23.6** | **56.5** | **18.5** |



https://dx.doi.org/10.1021/acssuschemeng.0c01571
ACS Sustainable Chem. Eng. 2020, 8, 8279−8287

induction temperature) of lignin−polyethylene blends. It is worth noticing that the fractions at lower molecular weight (below 2000 g/mol) are responsible, for at least 90% contribution of the whole OIT, and this is true for all the lignin examined. Anyway, among the four samples, the most interesting were the SWK and SG lignins that, showing the highest OIT values, provide the best performance allowing for the use of a reduced amount of lignin in the composite. An experimental confirmation of those observation could be found in Barana et al.[25] where the performance at break of fractionated SWK lignin−natural rubber composites were correlated to their phenol content.

## CONCLUSIONS

To conclude, this analytical approach opens several future perspectives. In theory, this approach could be applied to every lignin preparation. Moreover, other characteristic functional groups of lignin, such as alcohols and carboxylic acid, could be investigated to establish a complete correlation between functional groups and molecular weight. The main goal is to build structure−property application relationships (SPARs) required for any future large-scale application of technical lignins.

## ASSOCIATED CONTENT

### Supporting Information

The Supporting Information is available free of charge at https://pubs.acs.org/doi/10.1021/acssuschemeng.0c01571.

Model compounds' $^{1}H$, $^{13}C$, and $^{31}P$ NMR characterization, $^{31}P$ NMR spectra of reference (black line) and dansylated (red line) lignins, excitation and emission spectra of dansylated lignins, correlation between dansylated lignin fluorescence and total phenol content, GPC chromatograms of acetylated reference lignins and dansylated lignins (UV and fluorescence profiles) (PDF)

## AUTHOR INFORMATION


### Corresponding Author

**Marco Orlandi** − *Department of Earth and Environmental Sciences, University of Milano-Bicocca, Milan I-20126, Italy;* orcid.org/0000-0002-3787-5834; Phone: +39 02 6448 2919; Email: marco.orlandi@unimib.it

### Authors

**Anika Salanti** − *Department of Earth and Environmental Sciences, University of Milano-Bicocca, Milan I-20126, Italy*

**Luca Zoia** − *Department of Earth and Environmental Sciences, University of Milano-Bicocca, Milan I-20126, Italy;* orcid.org/0000-0002-0125-6476

Complete contact information is available at: https://pubs.acs.org/10.1021/acssuschemeng.0c01571


### Notes

The authors declare no competing financial interest.

## REFERENCES


(1) Gellerstedt, G.; Henriksson, G. Lignins: Major Sources, Structure and Properties. *Monomers, Polymers and Composites from Renewable Resources* **2008**, 201−224.

(2) PR Newswire. *Global Lignin Products Market - Segmented By Product Type, Source, Application, And Geography - Trends And Forecasts (2015-2020) - Reportlinker Review*. 2015.https://www.prnewswire.com/news-releases/global-lignin-products-market---segmented-by-product-type-source-application-and-geography---trends-and-forecasts-2015-2020---reportlinker-review-300145371.html.

(3) Del Río, J. C.; Rencoret, J.; Prinsen, P.; Martínez, Á. T.; Ralph, J.; Gutiérrez, A. Structural Characterization of Wheat Straw Lignin as Revealed by Analytical Pyrolysis, 2D-NMR, and Reductive Cleavage Methods. *J. Agric. Food Chem.* **2012**, *60* (23), 5922−5935.

(4) Crestini, C.; Lange, H.; Sette, M.; Argyropoulos, D. S. On the Structure of Softwood Kraft Lignin. *Green Chem.* **2017**, *19* (17), 4104−4121.

(5) LUNDQUIST, K.; KIRK, T. K. Fractionation-Purification of an Industrial Kraft Lignin. *Tappi* **1980**, *63* (1), 80−82.

(6) Costa, C. A. E.; Pinto, P. C. R.; Rodrigues, A. E. Lignin Fractionation from E. Globulus Kraft Liquor by Ultrafiltration in a Three Stage Membrane Sequence. *Sep. Purif. Technol.* **2018**, *192* (June 2017), 140−151.

(7) Zinovyev, G.; Sumerskii, I.; Korntner, P.; Sulaeva, I.; Rosenau, T.; Potthast, A. Molar Mass-Dependent Profiles of Functional Groups and Carbohydrates in Kraft Lignin. *J. Wood Chem. Technol.* **2017**, *37* (3), 171−183.

(8) Toledano, A.; Serrano, L.; Garcia, A.; Mondragon, I.; Labidi, J. Comparative Study of Lignin Fractionation by Ultrafiltration and Selective Precipitation. *Chem. Eng. J.* **2010**, *157* (1), 93−99.

(9) Boeriu, C. G.; Fiţigău, F. I.; Gosselink, R. J. A.; Frissen, A. E.; Stoutjesdijk, J.; Peter, F. Fractionation of Five Technical Lignins by Selective Extraction in Green Solvents and Characterisation of Isolated Fractions. *Ind. Crops Prod.* **2014**, *62*, 481−490.

(10) Wang, K.; Xu, F.; Sun, R. Molecular Characteristics of Kraft-AQ Pulping Lignin Fractionated by Sequential Organic Solvent Extraction. *Int. J. Mol. Sci.* **2010**, *11* (8), 2988−3001.

(11) Rohde, V.; Böringer, S.; Tübke, B.; Adam, C.; Dahmen, N.; Schmiedl, D. Fractionation of Three Different Lignins by Thermal Separation Techniques-A Comparative Study. *GCB Bioenergy* **2019**, *11* (1), 206−217.

(12) Ajao, O.; Jeaidi, J.; Benali, M.; Abdelaziz, O. Y.; Hulteberg, C. P. Green Solvents-Based Fractionation Process for Kraft Lignin with Controlled Dispersity and Molecular Weight. *Bioresour. Technol.* **2019**, *291* (May), 121799.

(13) Cui, C.; Sun, R.; Argyropoulos, D. S. Fractional Precipitation of Softwood Kraft Lignin: Isolation of Narrow Fractions Common to a Variety of Lignins. *ACS Sustainable Chem. Eng.* **2014**, *2* (4), 959−968.

(14) Jääskeläinen, A. S.; Liitiä, T.; Mikkelson, A.; Tamminen, T. Aqueous Organic Solvent Fractionation as Means to Improve Lignin Homogeneity and Purity. *Ind. Crops Prod.* **2017**, *103*, 51−58.

(15) Jiang, X.; Savithri, D.; Du, X.; Pawar, S.; Jameel, H.; Chang, H. M.; Zhou, X. Fractionation and Characterization of Kraft Lignin by Sequential Precipitation with Various Organic Solvents. *ACS Sustainable Chem. Eng.* **2017**, *5* (1), 835−842.

(16) Salanti, A.; Zoia, L.; Orlandi, M. Chemical Modifications of Lignin for the Preparation of Macromers Containing Cyclic Carbonates. *Green Chem.* **2016**, *18* (14), 4063−4072.

(17) Zoia, L.; Salanti, A.; Tolppa, E. L.; Ballabio, D.; Orlandi, M. Valorization of Side-Streams from a SSF Biorefinery Plant: Wheat Straw Lignin Purification Study. *BioResources* **2016**, *12* (1), 1680−1696.

(18) Bruschi, M.; Orlandi, M.; Rindone, B.; Rummakko, P.; Zoia, L. Asymmetric Biomimetic Oxidations of Phenols Using Oxazolidines as Chiral Auxiliaries: The Enantioselective Synthesis of (+)- and (−)-Dehydrodiconiferyl Alcohol. *J. Phys. Org. Chem.* **2006**, *19* (8−9), 592−596.

(19) Cruces-Blanco, C.; Segura Carretero, A.; Fernandez Peinado, S.; Fernandez Gutierrez, A. Spectrofluorimetric Determination of Methyl Paraben in Pharmaceutical Preparations by Means of Its Dansyl Chloride Derivative. *Microchim. Acta* **2000**, *134* (1−2), 107−111.

(20) Evdokimov, A. N.; Kurzin, A. V.; Fedorova, O. V.; Lukanin, P. V.; Kazakov, V. G.; Trifonova, A. D. Desulfurization of Kraft Lignin. *Wood Sci. Technol.* **2018**, *52* (4), 1165−1174.

(21) Albinsson, B.; Li, S.; Lundquist, K.; Stomberg, R. The Origin of Lignin Fluorescence. *J. Mol. Struct.* **1999**, *508* (1−3), 19−27.

(22) Granata, A.; Argyropoulos, D. S. 2-Chloro-4,4,5,5-Tetramethyl-1,3,2-Dioxaphospholaan Reagent for the Accurate Determination of the Uncondensed and Condensed Phenolic Moieties in Lignins. *J. Agric. Food Chem.* **1995**, *43*, 1538−1544.
(23) Lahtinen, M.; Heinonen, P.; Oivanen, M.; Karhunen, P.; Kruus, K.; Sipilä, J. On the Factors Affecting Product Distribution in Laccase-Catalyzed Oxidation of a Lignin Model Compound Vanillyl Alcohol: Experimental and Computational Evaluation. *Org. Biomol. Chem.* **2013**, *11* (33), 5454−5464.
(24) Salanti, A.; Orlandi, M.; Tolppa, E. L.; Zoia, L. Oxidation of Isoeugenol by Salen Complexes with Bulky Substituents. *Int. J. Mol. Sci.* **2010**, *11* (3), 912−926.
(25) Barana, D.; Orlandi, M.; Zoia, L.; Castellani, L.; Hanel, T.; Bolck, C.; Gosselink, R. Lignin Based Functional Additives for Natural Rubber. *ACS Sustainable Chem. Eng.* **2018**, *6* (9), 11843−11852.
(26) Domínguez-Robles, J.; Tamminen, T.; Liitiä, T.; Peresin, M. S.; Rodríguez, A.; Jääskeläinen, A. S. Aqueous Acetone Fractionation of Kraft, Organosolv and Soda Lignins. *Int. J. Biol. Macromol.* **2018**, *106*, 979−987.
(27) Lancefield, C. S.; Wienk, H. J.; Boelens, R.; Weckhuysen, B. M.; Bruijnincx, P. C. A. Identification of a Diagnostic Structural Motif Reveals a New Reaction Intermediate and Condensation Pathway in Kraft Lignin Formation. *Chem. Sci.* **2018**, *9* (30), 6348−6360.
(28) Wolter, K. Lignins: Occurrence, Formation, Structure and Reactions. *Forest Science* **1973**, *19*, 160.
(29) Wang, G.; Chen, H. Fractionation and Characterization of Lignin from Steam-Exploded Corn Stalk by Sequential Dissolution in Ethanol-Water Solvent. *Sep. Purif. Technol.* **2013**, *120*, 402−409.
(30) Arshanitsa, A.; Ponomarenko, J.; Dizhbite, T.; Andersone, A.; Gosselink, R. J. A.; Van Der Putten, J.; Lauberts, M.; Telysheva, G. Fractionation of Technical Lignins as a Tool for Improvement of Their Antioxidant Properties. *J. Anal. Appl. Pyrolysis* **2013**, *103*, 78−85.
(31) Barana, D.; Ali, S. D.; Salanti, A.; Orlandi, M.; Castellani, L.; Hanel, T.; Zoia, L. Influence of Lignin Features on Thermal Stability and Mechanical Properties of Natural Rubber Compounds. *ACS Sustainable Chem. Eng.* **2016**, *4* (10), 5258−5267.
(32) Sadeghifar, H.; Argyropoulos, D. S. Correlations of the Antioxidant Properties of Softwood Kraft Lignin Fractions with the Thermal Stability of Its Blends with Polyethylene. *ACS Sustainable Chem. Eng.* **2015**, *3* (2), 349−356.


https://dx.doi.org/10.1021/acssuschemeng.0c01571
*ACS Sustainable Chem. Eng.* 2020, 8, 8279−8287